The Journal of Phytopharmacology 2025; 14(6):411-421
Online at: www.phytopharmajournal.com

Research Article

ISSN 2320-480X
JPHYTO 2025; 14(6): 411-421
November- December
Received: 29-09-2025
Accepted: 15-01-2026
Published: 30-01-2026

doi: 10.31254/phyto.2025.14601

Millenium Vanlalpeka
Department of Zoology, Mizoram University (A Central University), Aizawl- 796004, Mizoram, India

Lal Fakawmi
Department of Zoology, Mizoram University (A Central University), Aizawl- 796004, Mizoram, India

Lal Dinpuii
Department of Zoology, Mizoram University (A Central University), Aizawl- 796004, Mizoram, India

Yasangam Umbon
Department of Pharmaceutical Sciences, Dibrugarh University, Dibrugarh-786004, Assam, India

Lalchhandami Tochhawng
Mizoram Science, Technology and Innovation Council, Government of Mizoram Aizawl- 796001, Mizoram, India

Liansangmawii Chhakchhuak
Department of Biotechnology, Pachhunga University College, Mizoram University (A Central University), Aizawl- 796001, Mizoram, India

Zothan Siama
Department of Zoology, Mizoram University (A Central University), Aizawl- 796004, Mizoram, India

Correspondence:
Dr. Zothan Siama
Department of Zoology, Mizoram University (A Central University), Aizawl- 796004, Mizoram, India
Email: zothans@gmail.com

In-vitro, *ex-vivo*, and *in-silico* assessment of the antioxidative potential of the leaf of the aromatic plant, *Homalomena aromatica* Schott

*Millenium Vanlalpeka, Lal Fakawmi, Lal Dinpuii, Yasangam Umbon, Lalchhandami Tochhawng, Liansangmawii Chhakchhuak, Zothan Siama**

ABSTRACT

Background: *Homalomena aromatica* Schott is a medicinal plant traditionally used for therapeutic purposes and known to contain diverse bioactive phytochemicals. Despite its ethnomedicinal relevance, comprehensive evaluation of its antioxidant efficacy and underlying molecular mechanisms remains limited. **Objective:** This study investigated the phytochemical profile and antioxidative potential of *H. aromatica* extracts. **Materials and Methods:** Antioxidant activity was assessed by DPPH, ABTS•+, and superoxide anion scavenging assays, along with reducing power based on Fe^{3+} to Fe^{2+} conversion. Protective effects against oxidative damage were further evaluated by erythrocyte hemolysis and lipid peroxidation inhibition in the liver of mice. Phytochemical profiling of the methanolic extract was conducted using LC–HRMS. Network pharmacology analysis was performed to identify key molecular targets, followed by molecular docking to assess ligand–target interactions. **Results:** The methanolic extract exhibited the highest phenolic and flavonoid contents, corresponding to superior radical scavenging and reducing activities. In contrast, the aqueous extract demonstrated the greatest efficacy in preventing hemolysis and lipid peroxidation. LC–HRMS analysis of the methanolic extract of *H. aromatica* (HAME) identified 24 major secondary metabolites. Network pharmacology highlighted glycogen synthase kinase-3β (GSK3B) as a key molecular target of these compounds. Notably, molecular docking revealed that 2,6-dihydroxy-7-methoxy-1,1,4a-trimethyl-3,4,10,10a-tetrahydro-2H-phenanthren-9-one showed strong binding affinity (−8.0 kcal/mol) toward GSK3B. **Conclusions:** *H. aromatica* extracts, particularly the methanolic fraction, possess high antioxidative capacity attributed to diverse phytochemicals. Furthermore, the identification of a potential GSK3B inhibitor underscores the therapeutic promise of this plant in the management of oxidative stress–related disorders.

Keywords: *Homalomena aromatica*, Phytochemicals, Free radicals, Antioxidant activity, Molecular docking.

INTRODUCTION

Free radicals are unstable and highly reactive species with unpaired valence electrons. At controlled levels, reactive oxygen species like $O_2^{\cdot-}$, H_2O_2, $^{\cdot}OH$, and $^1O_2$ contribute to host defense, vascular regulation, and intracellular signaling [1]. However, their excessive accumulation disrupts redox balance, causing oxidative stress, which is the imbalance between antioxidants and oxidants. Such stress may also emanate from external factors and has been linked to the development of a range of chronic and degenerative diseases, including autoimmune disorders, cancer, age-related diseases, cataracts, cardiovascular diseases, rheumatoid arthritis, and neurodegenerative diseases [2]. The body possesses exceptionally effective endogenous antioxidants, protecting the organisms from reactive oxygen species. They donate electrons to free radicals, rendering them harmless and neutralizing them by limiting oxidative damage in biological processes. While synthetic antioxidants are effective, their toxicity and carcinogenicity limit their use. Thus, natural antioxidants are preferred as safer alternatives with strong potential against oxidative damage [1].

Plant-derived antioxidants, mainly secondary metabolites, show protective effects against oxidative stress. They stimulate the immune system, block the formation of carcinogens, reduce oxidation, slow the growth rate of cancer cells, reduce inflammation, trigger apoptosis, prevent DNA damage, and regulate hormones such as estrogen and insulin, which are associated with an increased risk of breast and colon cancer [3]. Medicinal and Aromatic Plants (MAPs) are valued for their phytochemical-based therapeutic uses. *Homalomena aromatica* Schott, belonging to the family Araceae, is a rhizomatous herb native to Northeast India, known as “Sugandhimantri” and “Anchiri” in Mizo, possesses notable

medicinal and aromatic properties [4]. In traditional medicine, *H. aromatica* has been used for the treatment of several diseases [5]. Its rhizomes, along with the leaves, also possess several pharmacological applications [6,7]. Thus, this study evaluated *H. aromatica* leaf extracts for their antioxidant activity using *in vitro* and *ex vivo* models. LC–HRMS identified phytochemicals in the methanolic extract, while network pharmacology and molecular docking revealed molecular targets, highlighting potential drug candidates for oxidative stress–related disorders.

MATERIAL AND METHODS

Chemicals

Gallic acid, rutin hydrate, ferric chloride, Sodium nitrite, Nitro blue tetrazolium (NBT), 2-deoxyribose, 2,2'-azino-bis-(3-ethylbenzothiazoline-6- sulfonic acid) (ABTS), disodium hydrogen phosphate, potassium persulfate, Dimethyl sulfoxide (DMSO), potassium chloride, methanol, and hydrogen peroxide (H_2O_2) were obtained from HiMedia Laboratories Pvt., Ltd. (Mumbai, India). Glacial acetic acid, sulphuric acid, hydrochloric acid, and 1,1-diphenyl-2-picrylhydrazyl radicals (DPPH) were obtained from Sigma Aldrich Inc (Louis, Germany). Folin-ciocalteu's reagent, sodium hydroxide, sodium carbonate, Ascorbic acid, and Trichloroacetic acid (TCA) were obtained from SD fine-chem Ltd. (Mumbai, India). Aluminum chloride, potassium iodide, bismuth nitrate, sodium dihydrogen phosphate monohydrate, potassium dihydrogen phosphate, and sodium chloride were obtained from Merck Specialities Pvt., Ltd. (Mumbai, India). Potassium ferricyanide was obtained from Loba Chemie Pvt., Ltd. (Mumbai, India).

Collection of plant material and preparation of extracts

H. aromatica leaves were collected from Mamit, Mizoram, India. Before further processing, the leaves were thoroughly cleaned, dried, and minced. The leaves were shade-dried, powdered, and extracted using chloroform, methanol, and distilled water using soxhlet apparatus (40–60 cycles). The extracts were then filtered (Whatman No.1), concentrated by rotary evaporator at 40 °C, freeze-dried, and stored at −20 °C for further analysis.

Qualitative phytochemical analysis

The presence of various phytochemicals was screened for their presence in *H. aromatica* chloroform extract (HACE), *H. aromatica* methanolic extract (HAME), *H. aromatica* aqueous extract (HAAE), using standard protocols [8, 9].

Quantitative estimation of phytochemicals

Total phenolic content and total flavonoid content

Total phenolic content of *H. aromatica* extracts (HACE, HAAE, HAME) was determined following standard method [10]. *H. aromatica* extracts (1–8 mg/ml) were mixed with ten-fold diluted Folin–Ciocalteu reagent (5 ml) and sodium carbonate (4 ml, 0.115 mg/ml), incubated in the dark for 2 h, and absorbance was measured at 765 nm. Gallic acid (1–8 mg/ml) served as a standard for calibration, and phenolic content was expressed as gallic acid equivalents (GAE) in mg/g dry extract for each extract. Total flavonoid content of *H. aromatica* extracts was determined using the standard method [11]. Extracts (1–8 mg/ml) or rutin standard were mixed with distilled water, followed by 5% $NaNO_2$ and 10% $AlCl_3$ solutions, incubated, then 1 M NaOH was added, and the volume was adjusted to 2.5 ml. Absorbance was measured at 510 nm, and flavonoid content was expressed as rutin equivalent (RE mg/g extract).

In vitro antioxidant ass

DPPH radical scavenging activity

DPPH radical scavenging activity of *H. aromatica* extracts was assessed using a standard method [12] with slight modifications. Extracts (0.05–5 mg/ml) were mixed with 0.1 M DPPH solution and incubated in the dark for 30 min, and absorbance was measured at 523 nm. Antioxidant activity was expressed as IC_{50} and compared to ascorbic acid.

$$Scavenging\ \% = \frac{A\ blank - A\ sample}{A\ blank} x\ 100$$

Where A_{blank} is the absorbance of the control (all reagents except the test compound), and A_{sample} is the absorbance of the test compound.

ABTS radical scavenging activity.

ABTS radical scavenging activity of *HA* extracts was evaluated following a previous method [13]. $ABTS^+$ radicals were generated by mixing 7 mM ABTS and 2.45 mM potassium persulfate and incubated 12 h in the dark. Extracts (0.25–5 mg/ml) were mixed with ABTS working solution, absorbance was measured at 745 nm, and compared to ascorbic acid. The scavenging activity was then calculated using the formula:

$$Scavenging\ \% = \frac{A\ blank - A\ sample}{A\ blank} x\ 100$$

Where A_{blank} is the absorbance of the control reaction (all reagents except the test compound) and A_{sample} is the absorbance of the test compound.

Superoxide radical scavenging activity

Superoxide scavenging activity of *H. aromatica* extracts was measured using a modified nitro-blue tetrazolium (NBT) reduction method [14]. Reaction mixtures contained NBT, *H. aromatica* extracts (0.25–5 mg/ml), and alkaline DMSO, with absorbance recorded at 560 nm. DMSO served as a blank, ascorbic acid as a standard, and the scavenging activity was calculated using the formula:

$$Scavenging\ \% = \frac{Ae - Ao}{Ae}\ x\ 100$$

Where A_e represents absorbance with the sample and A_o represents absorbance without the sample.

Reducing power

Reducing power of *H. aromatica* extracts was assessed using standard method [15]. Extracts (0.25–5 mg/ml) were mixed with phosphate buffer and potassium ferricyanide, incubated 20 min at 50 °C, followed by TCA addition and centrifugation. Supernatant was then mixed with ferric chloride, and the absorbance was measured at 700 nm.

Ex-vivo antioxidant assay

Anti-hemolytic activity

The antioxidative potential of *H. aromatica* extracts was evaluated via inhibition of mice erythrocyte hemolysis [16]. Blood from Swiss albino mice was collected, and hemolysis was induced using H_2O_2. A 5% (v/v) suspension of RBC in phosphate-buffered saline (PBS) was incubated with *H. aromatica* extracts (7.5–20 mg/ml) at 37 °C for 3 h, and then diluted with PBS and again centrifuged at 2000 rpm for 10 minutes, and absorbance of the supernatant was measured at 540 nm to assess hemolysis inhibition. The inhibition rate was then calculated using the formula:

$$Inhibition\ rate\ (\%) = \frac{1 - (A1 - A2)}{Ao} x\ 100$$

Where A_0 is the absorbance of the control (without sample), A_1 is the absorbance in the presence of extract, and A_2 is the absorbance without sample (RBC).

Lipid peroxidation inhibition assay

Lipid peroxidation inhibitory activity of *H. aromatica* extracts was measured in a $FeCl_2$-H_2O_2 induced lipid peroxidation in the liver of mice [17]. The liver was excised from Swiss albino mice, and 1% of liver homogenate was prepared and centrifuged at 3000 rpm at 4ºC for 10 min. 0.5 ml of the supernatant was then mixed with 0.25 ml each of 0.5 mol/L $FeCl_2$ and H_2O_2, along with different fractions of *H. aromatica* extracts (5-10 mg/ml), which was then incubated at 37ºC for 1 h. Absorbance was measured at 535 nm after incubation, and the rate of inhibition of lipid peroxidation was calculated using the formula:

$$Inhibition\ rate\ (\%) = \frac{1-(A1-A2)}{Ao} x\ 100$$

Where A_0 is the absorbance of the control (without extract), A_1 is the absorbance when extract is present, and A_2 is the absorbance in the absence of liver homogenate.

Liquid chromatography-mass spectrometry (LC-HRMS) analysis

LC-HRMS was used to identify bioactive secondary metabolites in HAME. Analysis employed an ACCUCORE HPLC (C18, 150 × 2.1 mm, 1.7 µm) coupled to a triple quadrupole mass spectrometer (ACQ-TQD-QBB1152) with ESI source. Spectra were acquired from 150–2000 m/z in positive and negative modes. Mobile phases A (water + 0.1% formic acid) and B (acetonitrile + 0.1% formic acid) were applied in a linear gradient, with 5 µl injection and 950 L/h flow. Data were processed using MassLynx™ and OpenLynx™.

ADME prediction and druglikeness analysis

ADME prediction was performed to evaluate the absorption, distribution, metabolism, and excretion of HAME phytocompounds. Canonical SMILES were retrieved from PubChem. Druglikeness and bioavailability were screened using SwissADME protocols (Lipinski, Ghose, Veber, Egan, Muegge). Phytocompounds meeting druglikeness criteria were further assessed for pharmacokinetic properties using pkCSM (https://biosig.lab.uq.edu.au/pkcsm/prediction), facilitating identification of therapeutically effective and safe candidates.

Network pharmacology screening for potential gene targets

Screening of potential targets and Protein-Protein Interaction (PPI) network construction and core target screening

Target proteins of selected phytocompounds were predicted using Swiss Target Prediction (https://www.swisstargetprediction.ch/), and antioxidant-related proteins were retrieved from GeneCards (https://www.genecards.org/). Common targets were identified with Jvenn (https://jvenn.toulouse.inrae.fr/app/index.html) and analyzed through STRING (https://string-db.org/) to construct a protein–protein interaction network. TSV files were imported into Cytoscape 3.10.2, where CytoHubba ranked hub proteins by degree centrality.

Molecular docking

The automated docking tool, AutoDock 4.2.4 (Trott and Olson, 2010), was used to dock the selected phytocompound with the possible protein targets.

Retrieval and preparation of target protein and retrieval and preparation of ligand

The target protein's 3D structure was retrieved from the RCSB PDB (https://www.rcsb.org). Water molecules and heteroatoms were removed, polar hydrogens added, and active site coordinates identified using Discovery Studio 4.1. Kollmann charges were applied via AutoDock Tools v1.5.6, and the protein was exported in PDBQT format for molecular docking. PubChem was then employed to download the 3D molecular structure of the selected phytocompound in SDF format and then translated to PDB format using Open Babel. Ligand preparation for each molecule was conducted by uploading it into the Autodock Vina tool. Rotational interactions were assessed and modified as Gasteiger charges and non-polar hydrogen atoms were inserted and exported in the PDBQT format.

Animal model

Animal experiments followed NIH guidelines and were approved by Mizoram University IAEC (MZU/IAEC/2023-24/04). Swiss albino mice were maintained at 25 ± 2 °C, 12/12 h light/dark, with free access to food and water.

Statistical analysis

Data are expressed as mean ± standard error of the mean (SEM). IC_{50} values were determined by plotting response against log doses using Graph pad prism ver. 6.0. Variations in phytochemical contents, free radical scavenging activities, and antioxidant assays among extracts were analyzed using one-way analysis of variance (ANOVA) followed by Tukey's multiple comparison test. Statistical and graphical analyses were performed with SPSS ver. 16.0 (SPSS Inc., Chicago, IL, USA) and Graph pad prism ver. 8.0, with $p < 0.05$ considered statistically significant.

RESULTS

Qualitative phytochemical analysis

Phytochemical screening of *H. aromatica* extracts revealed the presence of various phytochemicals, wherein phlobatannins were absent in all extracts (Table 1).

Quantitative estimation of phytochemicals

Total phenolic and flavonoid content

At 8 mg/ml, HAME showed significantly higher phenolic (6967.92 ± 97.508 mg GAE/g) and flavonoid (1503.27 ± 9.498 mg RE/g) contents ($p < 0.001$) than HAAE (2373.25 ± 58.933 mg GAE/g; 483.05 ± 6.264 mg RE/g) and HACE (1111.93 ± 28.449 mg GAE/g; 247.432 ± 15.087 mg RE/g), respectively (Figure 1a-d).

***In vitro* antioxidant assay**

Log-doses of various extracts of *H. aromatica* and standard ascorbic acid (ASA) were plotted against inhibition (%) of DPPH, ABTS$^{\cdot+}$, and $O_2^{\cdot-}$ radicals for the calculation of IC_{50} (Figure 2a–c). Among them, HAME showed the strongest activity with IC_{50} values of 0.243 ± 0.026, 0.557 ± 0.033, and 0.189 ± 0.019 mg/ml, respectively, which were significantly better than HACE (1.090 ± 0.019, 2.602 ± 0.041, 0.862 ± 0.013 mg/ml) and HAAE (0.519 ± 0.039, 1.103 ± 0.047, 0.460 ± 0.037 mg/ml) and comparable to ascorbic acid (0.274 ± 0.011, 0.653 ± 0.002, 0.270 ± 0.003 mg/ml) (Figure 2d–f). Similarly, HAME shows the highest reducing power at 5 mg/ml with a value of 1.813 ± 0.023 mg/ml, surpassing HACE (0.754 ± 0.009 mg/ml) and HAAE (1.144 ± 0.002 mg/ml), and comparable to ascorbic acid (1.632 ± 0.002 mg/ml) (Figure 3).

***Ex vivo* antioxidant assay**

HAAE, at 20 mg/ml, shows the highest ($p < 0.001$) inhibitory activity against erythrocyte hemolysis and lipid peroxidation at 10 mg/ml, with an inhibition rate of 76.13 % and 90.69 %, as compared to HACE (56.17 %, 65.62 %) and HAME (62.87 %, 83.97 %) (Figure

4ab), indicating the potent lipid peroxidation inhibition and antihemolytic activity of HAAE.

Liquid chromatography-mass spectrometry (LC-HRMS)

LC-HRMS analysis of the methanolic extract of *H. aromatica* (HAME) revealed various phytochemicals. Key parameters such as precise mass, retention time, m/z ratio, and molecular formulas of deprotonated molecules are presented in Table 2, providing a detailed chemical profile of HAME.

Druglikeness and ADME analysis of phytocompounds from methanolic extract of *H. aromatica* (HAME)

Among the 24 major phytocompounds identified in HAME, 18 compounds exhibited no violations of the druglikeness rules (Table 3). The physicochemical properties of the phytocompounds and oral availability charts are also demonstrated in the supplementary data. The ADMET properties of the selected phytocompounds were predicted using SwissADME and pkCSM online servers (Supplementary data).

Network pharmacology screening for potential gene targets

Common targets of 2,6-dihydroxy-7-methoxy-1,1,4a-trimethyl-3,4,10,10a-tetrahydro-2H-phenanthren-9-one, and antioxidant

Following drug-likeness and ADMET profiling, 2,6-dihydroxy-7-methoxy-1,1,4a-trimethyl-3,4,10,10a-tetrahydro-2H-phenanthren-9-one was chosen for subsequent in silico studies. The Swiss Target Prediction database was employed to identify 100 probable molecular targets for the compounds in the methanolic extract of *H. aromatica*. A total of 5,038 protein targets associated with antioxidants were retrieved and compiled from the GeneCard database. Mutual gene mapping between the predicted targets of *H. aromatica* phytocompounds and antioxidant-associated genes led to the identification of 75 overlapping genes (Figure 5a).

Analysis of protein-protein interaction (PPI) network

For PPI network analysis, the 75 protein targets were loaded into the STRING database. As shown in Figure 5b, the final network has 359 edges and nodes with an enrichment p-value < 1.0e-16. The network was then imported into Cytoscape software and analyzed by determining centrality and other metrics. The Cytohubba plug-in revealed the top ten genes, as depicted in Figure 5c. One of the top core gene targets for 2,6-dihydroxy-7-methoxy-1,1,4a-trimethyl-3,4,10,10a-tetrahydro-2H-phenanthren-9-one was GSK3B.

Molecular docking analysis

Molecular docking was performed to evaluate interactions between 2,6-dihydroxy-7-methoxy-1,1,4a-trimethyl-3,4,10,10a-tetrahydro-2H-phenanthren-9-one (CID 14191448) and GSK3B (PDB ID 8DJC) using AutoDock Vina. The grid box parameters are displayed in Table 4. Wherein 2,6-dihydroxy-7-methoxy-1,1,4a-trimethyl-3,4,10,10a-tetrahydro-2H-phenanthren-9-one exhibited strong binding to GSK3B's active site (−8.0 kcal/mol), comparable to standard quercetin (CID 5280343) (−8.2 kcal/mol). This indicates its potential as a GSK3B inhibitor (Figure 6 a&b).

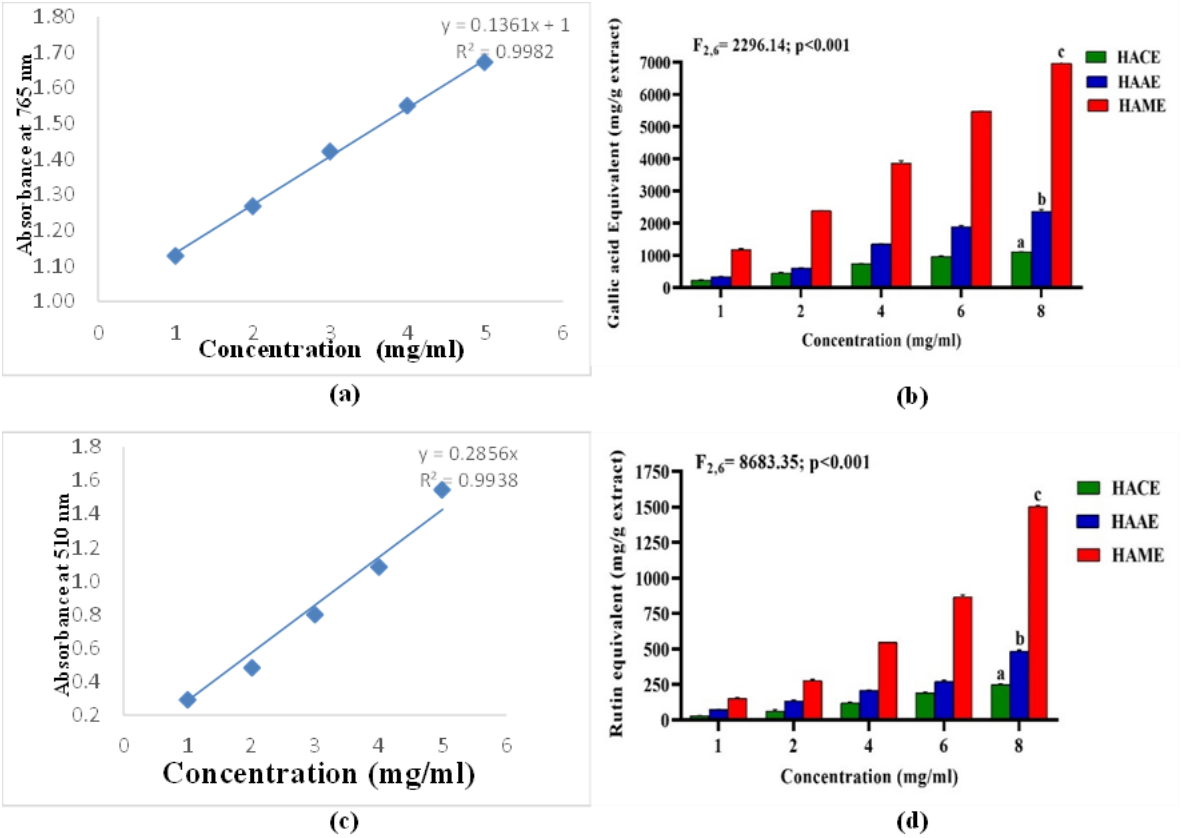

Figure 1: (a) Standard graph of gallic acid, (b) phenolic content of various extracts of *H. aromatica* determined as gallic acid equivalent, (c) Standard graph of rutin, (d) flavonoid content of various extracts of *H. aromatica* determined as rutin equivalent. HACE: *H. aromatica* chloroform extract; HAAE: *H. aromatica* aqueous extract; HAME: *H. aromatica* methanolic extract. Values are expressed as Mean ± SEM, n=3. Different letters indicate significant variation.

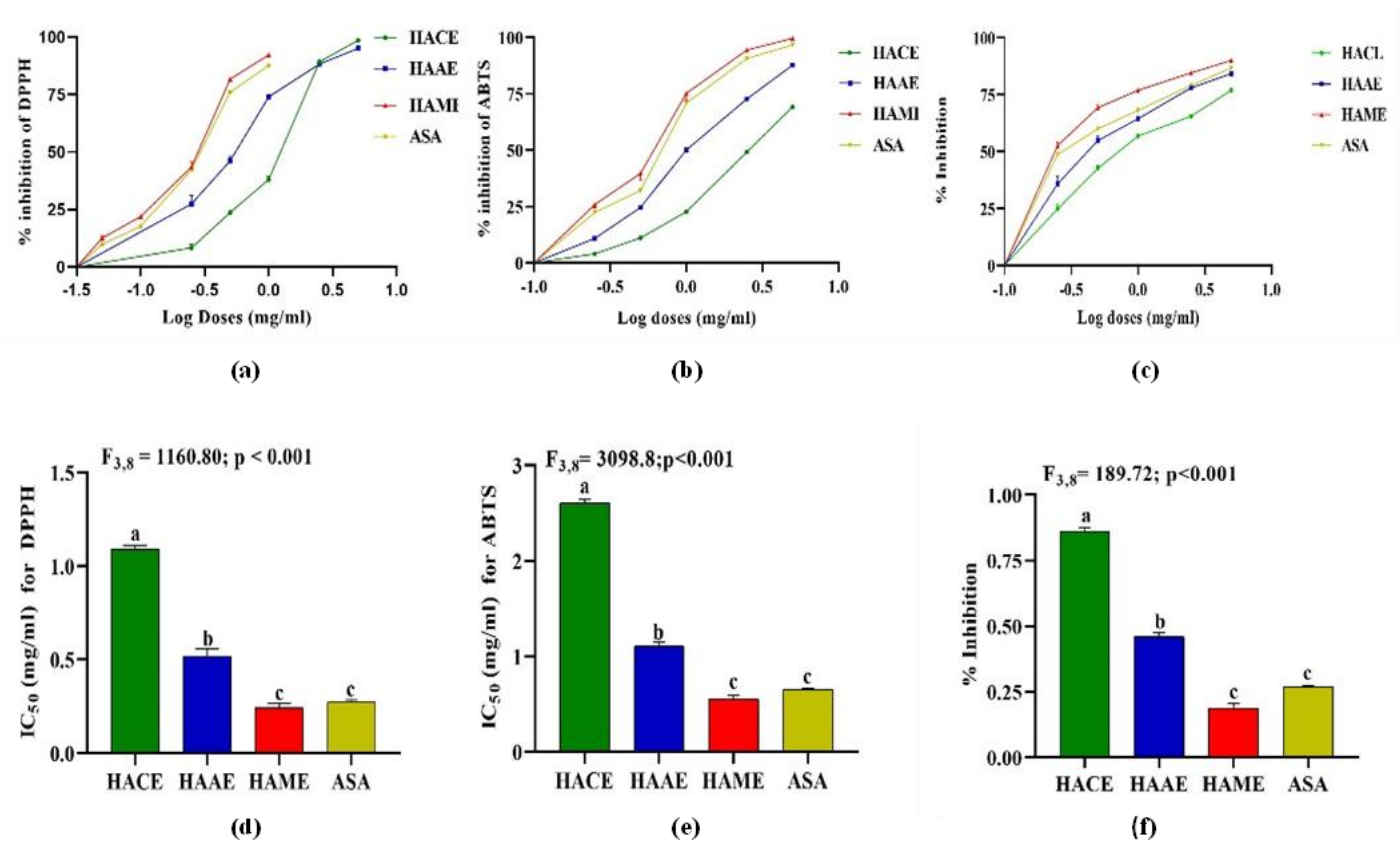

Figure 2: Plots of log-doses of HACE, HAAE, HAME, and ASA (ascorbic acid) against (a) DPPH, (b) ABTS, and (c) $O_2^{\bullet-}$ inhibition (%) for the calculation of IC_{50}. IC_{50} (mg/mL) of HACE, HAAE, HAME, and ASA for (d) DPPH, (e) ABTS, and (f) $O_2^{\bullet-}$. Values are expressed as Mean ± SEM, n = 3. Different letters indicate significant variation.

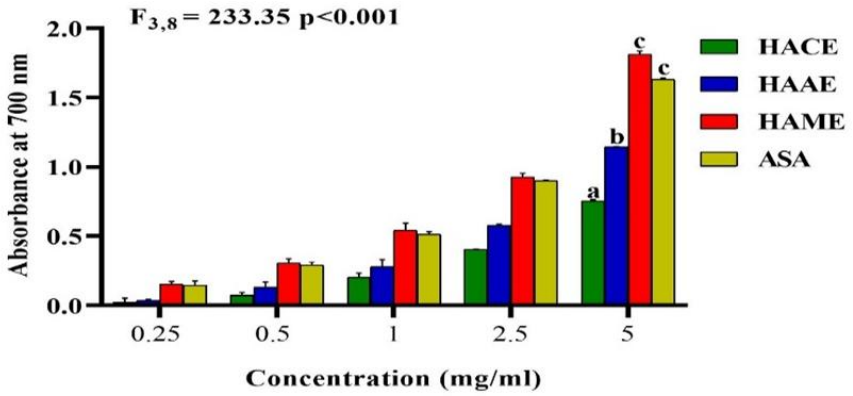

Figure 3. Reducing power of HACE, HAAE, HAME, and ASA at different concentrations. HACE: *H. aromatica* chloroform extract; HAAE: *H. aromatica* aqueous extract; HAME: *H. aromatica* methanolic extract; ASA: ascorbic acid (standard). Values are expressed as Mean ± SEM, n = 3. Different letters indicate significant variation

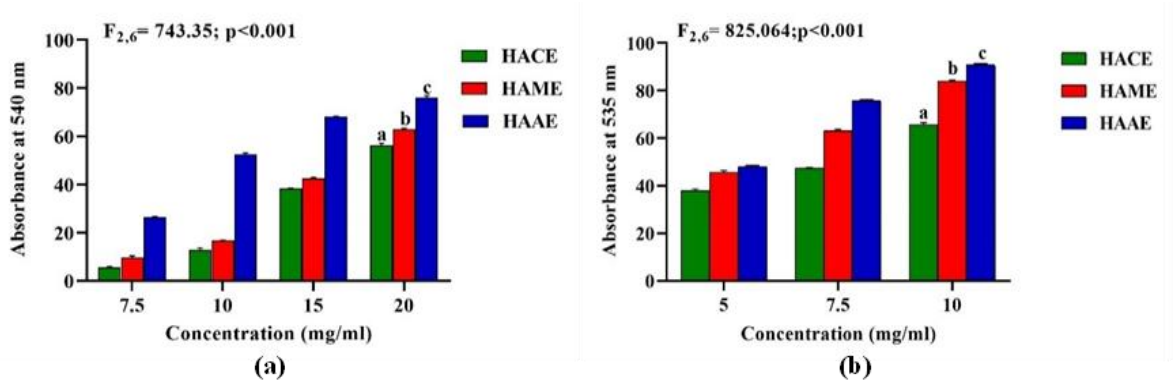

Figure 4: (a) Anti-hemolytic and (b) lipid peroxidation inhibition activity of various extracts of *H. aromatica*: HACE: *H. aromatica* chloroform extract; (b) HAME: *H. aromatica* methanolic extract; (c) HAAE: *H. aromatica* aqueous extract. Values are expressed as Mean ± SEM, n=3. Different letters indicate significant variation at $p < 0.001$.

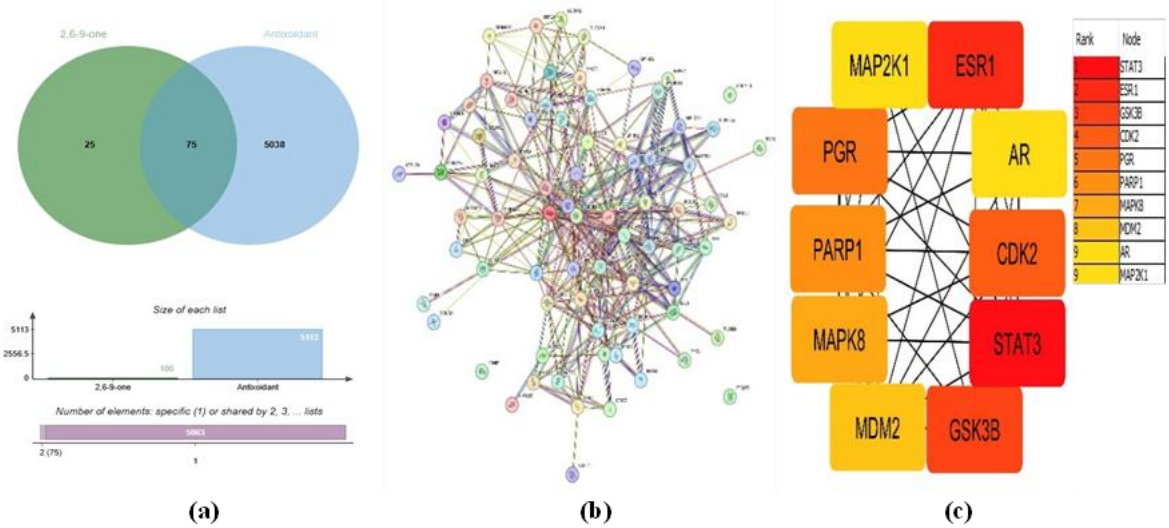

Figure 5: (a) Venn diagram of proteins involved in Antioxidants targeted by 2,6-dihydroxy-7-methoxy-1,1,4a-trimethyl-3,4,10,10a-tetrahydro-2H-phenanthren-9-one, (b) PPI Network of 75 protein targets of 2,6-dihydroxy-7-methoxy-1,1,4a-trimethyl-3,4,10,10a-tetrahydro-2H-phenanthren-9-one of HAME, (c) The top 10 potential targets network ranked of 2,6-dihydroxy-7-methoxy-1,1,4a-trimethyl-3,4,10,10a-tetrahydro-2H-phenanthren-9-one of HAME by degree value generated by 3.10.2.

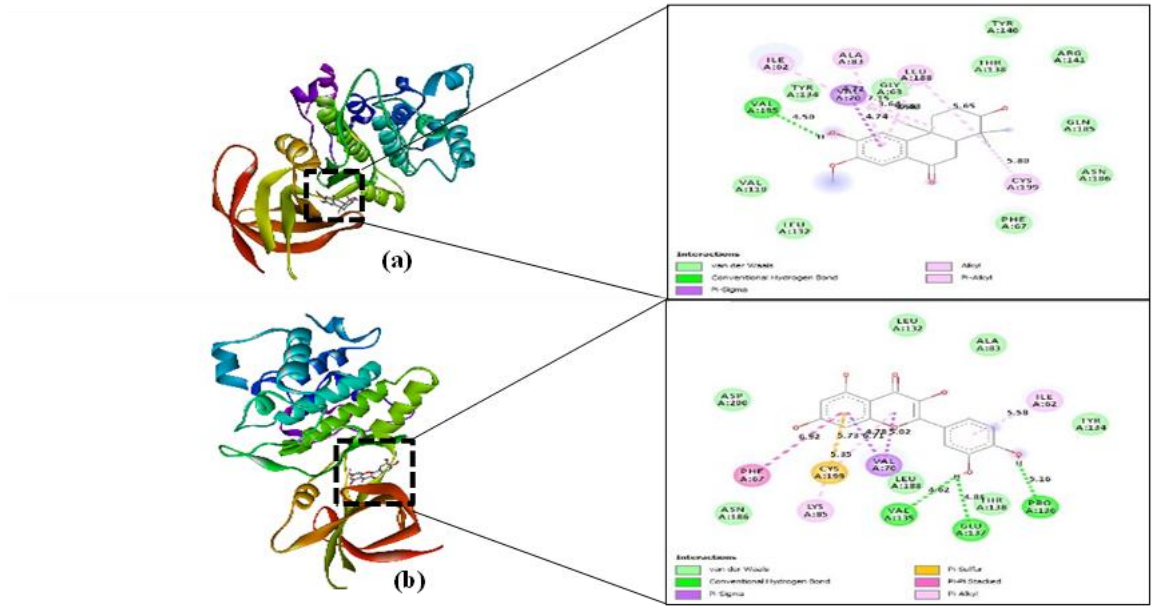

Figure 6: 3D structure of GSK3B showing the binding site and the main residues involved with ligands (a) 2,6-dihydroxy-7-methoxy-1,1,4a-trimethyl-3,4,10,10a-tetrahydro-2H-phenanthren-9-one and (b) standard quercetin.

Table 1: Phytochemical screening of various *H. aromatica* extracts. ('+' denotes the presence, and '–' denotes the absence of specific phytochemicals)

Phytochemical	Reagent	Colour Indication	HACE	HAAE	HAME
Alkaloids	Dragendroff's Reagent	Reddish brown precipitate	-	+	+
Cardiac Glycosides	Glacial Acetic Acid, Ferric Chloride, Sulphuric Acid	Brown Ring	-	-	-
Steroids	Sulphuric Acid	Red Colour	-	-	-
Saponins	Olive Oil	Whitish Emulsion	+	+	+
Tannins	Ferric Chloride	Brownish green or blue-black	-	-	+
Terpenoids	Sulphuric Acid	Reddish brown	-	+	+
Phlobatannins	Hydrochloric Acid	Red Precipitate	-	-	-

Table 2: Compounds identified in the methanolic extract of *H. aromatica* using LC-HRMS

Family	SI No	Compounds	Molecular weight	Retention Time	m/z ratio	Molecular Formula
Flavonoids	1	(2R)-5-methoxy-8,8-dimethyl-2-phenyl-2,3-dihydropyrano[2,3-h]chromen-4-one	336.38	27.311	337.14	$C_{21}H_{20}O_4$
Phenol	2	(3R)-3-(3,4-dimethoxyphenyl)-8-hydroxy-3,4-dihydroisochromen-1-one	300.30	27.744	301.11	$C_{17}H_{16}O_5$
	3	(7R,8R)-7,8-dihydroxy-3,5,7-trimethyl-8H-isochromen-6-one	222.24	28.512	223.25	$C_{12}H_{14}O_4$
	4	1-(3,4-dihydroxyphenyl)-6,7-dihydroxy-1,2-dihydronaphthalene-2,3-dicarboxylic acid	358.07	0.933	359.08	$C_{18}H_{14}O_8$
	5	2,6-dihydroxy-7-methoxy-1,1,4a-trimethyl-3,4,10,10a-tetrahydro-2H-phenanthren-9-one	304.39	23.473	305.18	$C_{18}H_{24}O_4$
	6	4-Hydroxyphenylethanol	138.17	24.357	139.08	$C_8H_{10}O_2$
	7	4-Methylcatechol	124.14	28.478	125.06	$C_7H_8O_2$
	8	(5R)-5-hydroxy-1-(4-hydroxy-3-methoxyphenyl)decan-3-one	294.39	28.412	295.19	$C_{17}H_{26}O_4$
	9	Roccellaric acid	332.3	24.558	333.10	$C_{17}H_{16}O_7$
Steroid	10	Calusterone	562.79	27.444	563.80	$C_{33}H_{54}O_7$
	11	Flurandrenolide	436.51	27.527	437.51	$C_{24}H_{33}FO_6$
Alkaloid	12	2-(hydroxymethyl)-4(3H)-quinazolinone	176.17	0.666	177.07	$C_9H_8N_2O_2$
Terpenoids	13	Ganoderic acid C1	560.73	29.162	561.74	$C_{32}H_{48}O_8$
	14	Phorbol 13-palmitate	592.89	29.674	593.89	$C_{36}H_{58}O_7$
Glycophospholipids	15	[3-(hexadecanoyloxy)-2-[icosa-5.8.11-trienoyloxy]propoxy]({[2.3.4.5.6-pentahydroxycyclohexyl]oxy})phosphinic acid	841.07	28.462	842.09	$C_{45}H_{81}O_{13}P$
Glycerolipids.	16	1-Monopalmitin	330.5	28.178	331.29	$C_{19}H_{38}O_4$
Aromatic ketones	17	Benzophenone-8	244.24	28.011	245.08	$C_{14}H_{12}O_4$
Aromatic alcohol	18	Benzyl alcohol	108.14	0.850	109.06	C_7H_8O
Propanoids	19	Cinnamic acid	148.16	29.880	149.06	$C_9H_8O_2$
Amino acids	20	L-Citrulline	175.18	27.544	176.10	$C_6H_{13}N_3O_3$
Acylglycine	21	N-Isobutyrylglycine	145.16	0.416	146.07	$C_6H_{11}NO_3$
Peptides	22	Bottromycin A2	839.45	29.146	833.51	$C_{42}H_{62}N_8O_7S$
Sulfonamides	23	Sulfaguanidine	214.25	0.783	215.26	$C_7H_{10}N_4O_2S$
Nucleoside	24	Uridine	44.2	26.059	245.08	$C_9H_{12}N_2O_6$

Table 3: Druglikeness analysis of drug candidates. 'Yes', indicate zero violation (A) (2R)-5-methoxy-8,8-dimethyl-2-phenyl-2,3-dihydropyrano[2,3-h] chromen-4-one (B) (3R)-3-(3,4-dimethoxyphenyl)-8-hydroxy-3,4-dihydroisochromen-1-one (C) (7R,8R)-7,8-dihydroxy-3,5,7-trimethyl-8H-isochromen-6-one (D) 1-(3,4-dihydroxyphenyl)-6,7-dihydroxy-1,2-dihydronaphthalene-2,3-dicarboxylic acid (E) 2,6-dihydroxy-7-methoxy-1,1,4a-trimethyl-3,4,10,10a-tetrahydro-2H-phenanthren-9-one (F) 4-Hydroxyphenylethanol (G) 4-Methylcatechol (H) (5R)-5-hydroxy-1-(4-hydroxy-3-methoxyphenyl) decan-3-one (I) Calusterone (J) Flurandrenolide (K) 2-(hydroxymethyl)-4(3H)-quinazolinone (L) Ganoderic acid C1 (M) 1-Monopalmitin (N) Benzophenone-8 (O) Benzyl alcohol (P) L-Citrulline (Q) Sulfaguanidine (R) Uridine

Rule	A	B	C	D	E	F	G	H	I	J	K	L	M	N	0	P	Q	R
Lipinski	Yes	Yes	Yes	Yes	Yes	Yes	Yes	Yes	Yes	Yes	Yes	Yes	Yes	Yes	Yes	Yes	Yes	Yes
Ghose	Yes	Yes	Yes	Yes	Yes	No	No	Yes	Yes	Yes	Yes	No	Yes	Yes	No	No	Yes	No
Veber	Yes	Yes	Yes	No	Yes	Yes	Yes	Yes	Yes	Yes	Yes	Yes	No	Yes	Yes	Yes	Yes	Yes
Egan	Yes	Yes	Yes	No	Yes	Yes	Yes	Yes	Yes	Yes	Yes	Yes	Yes	Yes	Yes	Yes	No	Yes
Muegge	Yes	Yes	Yes	No	Yes	No	No	Yes	Yes	Yes	No	Yes	No	Yes	No	No	Yes	Yes
Bioavailability score	0.55	0.55	0.55	0.11	0.55	0.55	0.55	0.55	0.55	0.55	0.55	0.56	0.55	0.55	0.55	0.55	0.55	0.55

Table 4: The dimension of the grid box for molecular docking of selected protein (GSK3B)

	Centre			Size			Exhaustiveness
Target Protein	X	Y	Z	X	Y	Z	
GSK3B	19.457167	-7.077289	85.984116	30	30	30	8

DISCUSSION

H. aromatica extracts contain various phytocompounds, and these polyphenolic phytochemicals are a vast source of novel drugs against various ailments with no adverse effects and exhibit antioxidant, anti-inflammatory, analgesic, antidiabetic, antimicrobial, and neuroprotective activities, regulate gene transcription, enhance immunity, and protect against lung and prostate tumors [18]. The total phenolic and flavonoid contents increased dose-dependently in *H. aromatic* extracts, wherein HAME shows the highest total flavonoids and phenolic content among all the extracts. Phenolic compounds, abundant in medicinal herbs and dietary plants, exhibit potent antioxidant activity via free radical scavenging and stabilization through conjugated aromatic systems and hydroxyl groups [19]. They even exhibit several pharmacological activities, including antimicrobial, antiallergenic, antithrombotic, anti-atherogenic, anti-inflammatory, vasodilatory, and cardioprotective effects [19,20]. Flavonoids similarly alleviate oxidative stress–related diseases through electron donation, oxidase inhibition, antioxidant enzyme activation, and metal chelation [6]. Their hydroxyl groups also enhance bioavailability and antioxidant activity. They also possess several pharmacological effects, such as anti-inflammatory, antibacterial, antiviral, anti-allergic, anti-aging, anticancer, neuroprotective, cardioprotective, immunomodulatory, antiparasitic, and antidiabetic properties [21].

Endogenous free radicals, produced during normal metabolism, are neutralized by antioxidant systems. Disruption leads to excess radicals, contributing to diseases such as inflammation, diabetes, neurodegeneration, cardiovascular disorders, and cancer. The extracts of *H. aromatica* exhibited concentration-dependent radical scavenging activity against DPPH, $ABTS^{+}$, and $O_2^{\cdot -}$ radicals. Similarly, reducing power increased dose-dependently, with HAME showing the highest value. The pronounced antioxidant potential of *H. aromatica* leaf extracts, demonstrated via radical-scavenging and reducing activities, highlights their phytopharmacological significance against oxidative stress–related disorders. This activity is attributed to electron-donating compounds, particularly phenolics, where hydroxyl groups and reduced –OH bond dissociation energy enhance free radical scavenging [22].

Red blood cells, rich in polyunsaturated fatty acids, are primary targets of free radicals, leading to oxidative damage and hemolysis [23]. Lipids are particularly susceptible to free radical–induced peroxidation, producing cytotoxic products such as malondialdehyde (MDA) and 4-hydroxynonenal, contributing to cancer, diabetes, inflammation, and cardiovascular diseases [24]. However, phenolic and flavonoid constituents of *H. aromatica* leaves protect erythrocytes by stabilizing membranes, scavenging free radicals, and inhibiting lipid peroxidation. Phenolics limit radical diffusion through membrane partitioning, while flavonoid hydroxyl groups enhance erythrocyte stability and reduce lipid peroxidation [25].

LC-HRMS is a powerful analytical technique widely used for the precise identification, quantification, and structural elucidation of complex chemical mixtures. The analysis revealed the presence of 24 major compounds in the methanolic extract of *H. aromatica*, where most of the compounds identified have been reported to possess several pharmacological activities. (3R)-3-(3,4-dimethoxyphenyl)-8-hydroxy-3,4-dihydroisochromen-1-one has been reported to possess anti-inflammatory, antiallergic, antioxidant, and anti-degranulation properties. The compound, (5R)-5-hydroxy-1-(4-hydroxy-3-methoxyphenyl) decan-3-one also possesses anti-inflammatory, antioxidant, anticancer, and anti-diabetic activity. Ganoderic acid C1 also possesses anticancer activity and multiple biological activities like anti-hypersensitive, anticancer, antiviral, analgesic, and anti-HIV-1. L-Citrulline also possesses anabolic, antidiabetic, and antiaging activity. Cinnamic acid also possesses several pharmacological properties, such as anticancer, neuroprotective, antidiabetic, anti-inflammatory, antimicrobial, and antioxidant [26-28].

Drug-likeness is an essential concept in drug discovery, as it reflects the likelihood that a compound possesses the physicochemical and structural features required for oral bioavailability and favorable pharmacokinetic behavior. Early evaluation of drug-likeness helps filter out molecules with poor absorption, distribution, metabolism, and excretion (ADME) properties, thereby reducing costly late-stage failures [29]. Thus, drug-likeness assessment is a critical step for improving efficiency and success rates in modern drug development. SwissADME was used to predict the physicochemical parameters and drug-likeness of phytocompounds derived from HAME, with drug-likeness examined through Lipinski, Ghose, Veber, Egan, and Muegge rules. Eighteen compounds exhibited no violations of the druglikeness rules. LogS predicts compound water solubility, influencing drug distribution; in HAME, benzyl alcohol is most soluble and 1-monopalmitin is least soluble. Caco-2 permeability and intestinal absorption were highest for (2R)-5-methoxy-8,8-dimethyl-2-phenyl-2,3-dihydropyrano[2,3-h] chromen-4-one (1.452) with an intestinal absorption score of (96.047 %), and lowest for N-isobutyrylglycine (-0.481) with an intestinal absorption score of (39.008 %). Volume of distribution analysis indicated that (3R)-3-(3,4-dimethoxyphenyl)-8-hydroxy-3,4-dihydroisochromen-1-one had low distribution (-0.102). The blood-brain barrier (BBB) regulates brain exposure to exogenous molecules, with logBB > 0.3 indicating permeation and < −1 indicating low likelihood. Among HAME compounds,(3R)-3-(3,4-dimethoxyphenyl)-8-hydroxy-3,4-dihydroisochromen-1-one may cross the BBB, while Bottromycin A2 is unlikely to penetrate the CNS. pkCSM analysis revealed two CYP3A4 substrates ((2R)-5-methoxy-8,8-dimethyl-2-phenyl-2,3-dihydropyrano[2,3-h] chromen-4-one and (3R)-3-(3,4-dimethoxyphenyl)-8-hydroxy-3,4-dihydroisochromen-1-one), no CYP2D6 substrates, and predicted all compounds as skin-safe with no AMES toxicity.

In-silico approaches, including network pharmacology and molecular docking, have enhanced the identification of disease-associated drug targets and therapeutic compounds [30]. GSK3B, a ubiquitous serine/threonine kinase, regulates metabolism and signaling; its dysregulation contributes to metabolic, neurological, oncological, aging-related, and immune disorders, highlighting its therapeutic significance [31]. The molecular docking study revealed that 2,6-dihydroxy-7-methoxy-1,1,4a-trimethyl-3,4,10,10a-tetrahydro-2H-phenanthren-9-one exhibits a high binding affinity for GSK3B, which renders it a suitable option for the development of next-generation GSK3B inhibitors.

CONCLUSION

The present study reveals that *H. aromatica* leaf extracts contain diverse phytochemicals and high polyphenol levels, contributing to potent antioxidant activity, demonstrated by dose-dependent scavenging of DPPH, ABTS, and $O_2^{\cdot -}$ radicals and ferric reducing power. The extracts also inhibited lipid peroxidation and hemolysis due to the high content of phenols and flavonoids in the extracts. Molecular docking indicated that the compound in the methanolic extract, particularly 2,6-dihydroxy-7-methoxy-1,1,4a-trimethyl-3,4,10,10a-tetrahydro-2H-phenanthren-9-one, targets GSK3B, highlighting its therapeutic potential against oxidative stress-related diseases and further highlights the importance of additional investigation of the compound 2,6-dihydroxy-7-methoxy-1,1,4a-trimethyl-3,4,10,10a-tetrahydro-2H-phenanthren-9-one as part of drug development processes.

Acknowledgments

We thank the Ministry of Tribal Affairs (Scholarship Division), Government of India, for providing NFST fellowships to Millenium

Vanlalpeka (202324-NFST-MIZ-01401), Lal Fakawmi (202122-NFST-MIZ-O2580), Lal Dinpuii (202324-NFST-MIZ-00950), Yasangam Umbon (202223-NFST-ARU-00552).

Conflict of interest

The authors declared no conflict of interest.

Financial Support

None declared.

ORCID ID

Millenium Vanlalpeka: https://orcid.org/0009-0001-0222-9496

Lal Fakawmi: https://orcid.org/0009-0001-7196-8209

Lal Dinpuii: https://orcid.org/0009-0000-6176-2752

Yasangam Umbon: https://orcid.org/0000-0001-9482-9917

Lalchhandami Tochhawng: https://orcid.org/0000-0002-3563-4850

Liansangmawii Chhakchhuak: https://orcid.org/0000-0002-8660-4221

Zothan Siama: https://orcid.org/0000-0003-0859-4109

REFERENCES

1. Gulcin İ. Antioxidants and antioxidant methods: An updated overview. Arch Toxicol. 2020;94(3):651-715.
2. Akbari B, Baghaei-Yazdi N, Bahmaie M, Mahdavi Abhari F. The role of plant-derived natural antioxidants in reduction of oxidative stress. Biofactors. 2022;48(3):611-633.
3. Nwozo OS, Effiong EM, Aja PM, Awuchi CG. Antioxidant, phytochemical, and therapeutic properties of medicinal plants: A review. Int J Food Prop. 2023;26(1):359-388.
4. Tiwari S, Upadhyay N, Singh BK, Singh VK, Dubey NK. Chemically characterized nanoencapsulated *Homalomena aromatica* Schott essential oil as green preservative against fungal and aflatoxin B1 contamination of stored spices. Environ Sci Pollut Res Int. 2022;29(2):3091-3106.
5. Roy SJ, Baruah PS, Lahkar L, Gurung L, Saikia D, Tanti B. Phytochemical analysis and antioxidant activities of *Homalomena aromatica* Schott. J Pharmacogn Phytochem. 2019;8(1):1379-1385.
6. Policegoudra RS, Goswami S, Aradhya SM, Chatterjee S, Datta S, Sivaswamy R, et al. Bioactive constituents of *Homalomena aromatica* essential oil and its antifungal activity. J Mycol Med. 2012;22(1):83-87.
7. Ali MS, Sayem SA, Habibullah, Quah Y, Lee EB, Birhanu BT, et al. Antioxidant, thrombolytic and neuropharmacological activities of *Homalomena aromatica* leaves. Molecules. 2021;26(4):975.
8. Harborne AJ. Phytochemical Methods: A Guide to Modern Techniques of Plant Analysis. London: Springer; 1998.
9. Doughari JH. Phytochemicals: Extraction Methods, Basic Structures and Mode of Action as Potential Chemotherapeutic Agents. Rijeka: InTech; 2012.
10. Singleton VL, Rossi JA. Colorimetry of total phenolics with phosphomolybdic–phosphotungstic acid reagents. Am J Enol Vitic. 1965;16(3):144-158.
11. Sakanaka S, Tachibana Y, Okada Y. Preparation and antioxidant properties of Japanese persimmon leaf tea. Food Chem. 2005;89(4):569-575.
12. Leong LP, Shui G. Antioxidant capacity of fruits in Singapore markets. Food Chem. 2002;76(1):69-75.
13. Re R, Pellegrini N, Proteggente A, Pannala A, Yang M, Rice-Evans C. Antioxidant activity using ABTS radical cation decolorization assay. Free Radic Biol Med. 1999;26(9-10):1231-1237.
14. Hyland K, Voisin E, Banoun H, Auclair C. Superoxide dismutase assay using alkaline dimethylsulfoxide. Anal Biochem. 1983;135(2):280-287.
15. Oyaizu M. Studies on antioxidative activities of browning reaction products from glucosamine. Jpn J Nutr Diet. 1986;44(6):307-315.
16. Li N, Alam J, Venkatesan MI, Eiguren-Fernandez A, Schmitz D, Di Stefano E, et al. Nrf2 regulates antioxidant defense against diesel exhaust chemicals. J Immunol. 2004;173(5):3467-3481.
17. Kaur R, Thukral AK, Arora S. Free radical attenuation by aqueous extract of *Chlorophytum borivilianum* tuber peels. J Chin Clin Med. 2010;5(1):1-7.
18. Lalremruati M, Lalmuansangi C, Siama Z. Antioxidative potential of *Mussaenda macrophylla* extracts. J Appl Pharm Sci. 2019;9(12):094-102.
19. de Alencar Silva A, Pereira-de-Morais L, da Silva RE, de Menezes Dantas D, Milfont CG, Gomes MF, et al. Pharmacological screening of caffeic acid. Chem Biol Interact. 2020;332:109269.
20. Sun W, Shahrajabian MH. Therapeutic potential of phenolic compounds in medicinal plants. Molecules. 2023;28:1845.
21. Dias MC, Pinto DC, Silva AM. Plant flavonoids: Chemical characteristics and biological activity. Molecules. 2021;26(17):5377.
22. Lalmuansangi C, Lalremruati M. Antioxidative potential of *Stemona tuberosa* tuber extracts. Curr Trends Biotechnol Pharm. 2020;14(3):347-358.
23. Khalili M, Ebrahimzadeh MA, Safdari Y. Antihemolytic activity of plant extracts in mouse erythrocytes. Arh Hig Rada Toksikol. 2014;65(4):399-405.
24. Badmus JA, Adedosu TO, Fatoki JO, Adegbite VA, Adaramoye OA, Odunola OA. Lipid peroxidation inhibition by *Mangifera indica* leaf fractions. Acta Pol Pharm. 2011;68(1):23-29.
25. Lalsangpuii F, Rokhum SL, Nghakliana F, Fakawmi L, Ruatpuia JV, Laltlanmawii E, et al. Green synthesis of silver nanoparticles using *Spilanthes acmella*. ACS Omega. 2022;7(48):44346-44359.
26. Chen Y, Yan T, Gao C, Cao W, Huang R. Natural products from the genus Tephrosia. Molecules. 2014;19(2):1432-58.
27. Paudel KR, Orent J, Penela OG. Pharmacological properties of ginger: Evidence from meta-analyses. Front Pharmacol. 2025;16:1619655.
28. Chauhan N. Pharmacological aspects of 6-gingerol: A review. Agric Sci Dig. 2022;42(5):528-533.
29. Jia CY, Li JY, Hao GF, Yang GF. A drug-likeness toolbox facilitates ADMET study. Drug Discov Today. 2020;25(1):248-258.
30. Yang L, Zhao Y, Xu H, Ma Y, Wang L, Ma J, et al. Network pharmacology-based mechanisms of He's Yangchao Formula. Evid Based Complement Alternat Med. 2022;2022:8361808.
31. McCubrey JA, Steelman LS, Bertrand FE, Davis NM, Abrams SL, Montalto G, et al. Roles of GSK-3 and Wnt/β-catenin in leukemogenesis. Leukemia. 2014;28:15-33.

HOW TO CITE THIS ARTICLE

Vanlalpeka M, Fakawmi L, DinpuiiL, Umbon Y, Tochhawng L, Chhakchhuak L, et al. *In-vitro*, *ex-vivo*, and *in-silico* assessment of the antioxidative potential of the leaf of the aromatic plant, *Homalomena aromatica* Schott. J Phytopharmacol 2025; 14(6):411-421. doi: 10.31254/phyto.2025.14601